Development of a Versatile Calibration Method for Electro-Magnetic Calorimeters Using a Stopped Cosmic-ray Beam

H. Ito, K. Horie, H. Kawai, S. Kodama, S. Shimizu for the J-PARC TREK collaboration

***Abstract*—A new method using a stopped cosmic-ray beam for the calibration of an electro-magnetic calorimeter which consists of several hundreds of modules has been established. Cosmic muons stop in the calorimeter, and positrons (and electrons) from the muon decays with the maximum energy of 53 MeV are used for the energy calibration. These events could be identified as double pulses observed by a flash ADC. This technique has many advantages, (1) intermediate energy scale (< 53 MeV) to interpolate between a few MeV for radioactive sources and 153 MeV, the muon from $K^+ \to \mu^+\nu_\mu$, (2) efficient procedure to calibrate all modules at the same time and (3) versatile method applied for many types of electro-magnetic calorimeters. This method was checked in the J-PARC E36 experiment which was performed to precisely measure the ratio of $\Gamma(K^+ \to e^+\nu_e)/\Gamma(K^+ \to \mu^+\nu_\mu)$. Double pulses from the CsI(Tl) photon detector were successfully observed and the waveform function was carefully studied to decompose the second pulse generated by the decay positron. The experimental energy spectrum is consistent with the simulated Michel spectrum taking into account the shower leakage from the CsI(Tl) module, which indicates the validity of the proposed calibration method.**

***Index Terms*—Electronic Magnetic Calorimeter, Energy Calibration, Cosmic-ray muons, Waveform Fitting, J-PARC**

I. Introduction

The J-PARC E36 experiment is searching for the lepton universality violation by a precise measurement of the ratio of the kaon semi-leptonic decay widths, $R_K = \Gamma(K^+ \to e^+\nu_e)/\Gamma(K^+ \to \mu^+\nu_\mu)$ at the Japan Proton Accelerator Research Complex (J-PARC) [1]. The experiment was performed using a stopped positive kaon beam in conjunction with the superconducting toroidal spectrometer. It has been well known that in the Standard Model (SM), the ${R_K}^{SM}$ ratio can be described as

$$\begin{aligned} {R_K}^{SM} &= \frac{{m_e}^2}{{m_\mu}^2}\left(\frac{{m_K}^2-{m_e}^2}{{m_K}^2-{m_\mu}^2}\right)^2(1+\delta_\gamma) \qquad (1)\\ &= (2.477 \pm 0.001)\times 10^{-5}, \end{aligned}$$

where m_x denotes the mass of the particles ($x = e,\ \mu,\ K$) and δ_γ presents an electromagnetic radiative correction [2], [3]. A deviation of the experimental R_K value from the SM prediction directly leads to lepton universality violation, indicating the contribution of new physics beyond the SM. Recently the NA62 experimental group reported the result of the R_K measurement as $(2.488 \pm 0.007\ (\mathrm{stat}) \pm 0.007\ (\mathrm{sys})) \times 10^{-5}$ ($\delta R_K/R_K \sim 0.4\%$) using an in-flight kaon method [4], which is complementary to the approach of the E36 experiment.

The detector for the J-PARC E36 experiment was developed by upgrading the detector system of the KEK-PS E246 experiment [5]. K_{l2} events were collected with the toroidal spectrometer which comprises an analyzing magnet with tracking devices and a segmented CsI(Tl) calorimeter. The toroidal spectrometer has 12 identical sectors with rotational symmetry of 30 degrees. The separated K^+ beam was tagged by a Fitch-type Cherenkov counter and stopped in an active target based on scintillating fibers with MPPC readouts. Charged particle momentum was determined by reconstructing the track using hit positions measured by a spiral fiber tracker made of 4-layer scintillating fiber ribbon windings (SFT) [7] and 3 multi-wire proportional chambers (C2, C3, and C4). The particle identification was performed by 3 independent systems a silica aerogel tiles (AC) Cherenkov counter [6], a time-of-flight measurement, and a lead-glass Cherenkov counter (PDG) [8]. In the E36 experiment, the spectrum distortion associated with detector misalignments can be eliminated due to the rotational symmetry structure of 12 identical gaps, and the systematic uncertainty was highly suppressed.

It should be emphasized that there are two radiative processes of $K^+ \to e^+\nu_e\gamma$ and their separation is very important because the internal bremsstrahlung (IB) decays have to be included in the R_K determination, while the structure dependence (SD) contributions are backgrounds and have to be subtracted. It is possible to separate the IB and SD processes by the spectroscopic studies using the e^+-γ correlation spectra due to the distinct structure of the two processes. Therefore, the photon measurement by the CsI(Tl) calorimeter is one of the key issues in the E36 experiment.

II. Calibration using Stopped Cosmic-ray muons

A new calibration method has been developed for electro-magnetic calorimeters using the endpoint energy of cosmic-ray muons in the decay spectrum ($\mu^+ \to e^+\nu_e\bar{\nu_\mu}$), which the muons stopped in the calorimeter crystals. This method has the following advantages: (1) intermediate energy scale (< 53 MeV) to interpolate between a few MeV for radioactive sources and 153 MeV for the muon from $\mathrm{K}^+ \to \mu^+\nu_\mu$, (2) efficient procedure to calibrate all modules at the same time without using accelerators and (3) versatile method applicable for many types of electro-magnetic calorimeters.

Manuscript received November 30, 2016;

H. Ito, H. Kawai and S. Kodama are with Graduate School of Science, Chiba University, 1-33, Yayoicho, Inage, Chiba, Japan (e-mail of corresponding author: hiroshi@hepburn.s.chiba-u.ac.jp).

K. Horie and S. Shimizu are with Graduate School of Science, Osaka University, 1-1, Machikaneyamacho, Toyonaka, Osaka, Japan

A. The CsI(Tl) Calorimeter

The calorimeter, a highly segmented assembly of 768 CsI(Tl) crystal modules, covered 75% of the total solid angle. There were 12 holes for the outgoing charged particles and 2 holes for the beam entrance and exit. Each crystal had a coverage of 7.5 degree along both the polar and azimuthal directions. The CsI(Tl) assembly had a size of 1.0 m in diameter and a length of 1.4 m [9]. The length of the CsI(Tl) modules was 25 cm (13.5 radiation length), which was enough to obtain sufficient energy resolution as well as to avoid nuclear counter effects. Since the CsI(Tl) calorimeter had to be operated under the relatively strong fringing field of the spectrometer where PMTs would be difficult to use, PIN photodiodes were employed to read out the scintillation light of the CsI(Tl) crystals. Each crystal with the associated PIN diode and the pre-amplifier was assembled in an Al container of 0.1 mm thickness. A charge sensitive pre-amplifier with a time constant of 600 μ sec and a gain of 0.5 V/pC was directly attached to the PIN diode. The output signal of the pre-amplifier was fed to a shaping amplifier with 0.5 μ sec time constant. The energy and timing were measured by recording the waveform of the shaping amplifier output data with a flash ADC, VF48 (25 MHz) manufactured at TRIUMF.

B. Calibration method

Although a calibration method using cosmic-ray muons has been well established, the essential point of the proposed method is the use of stopped muons in the CsI(Tl) calorimeter. This method was performed by comparing the experimental data compared with the Monte Carlo simulation. In the simulation, the energy deposit in the CsI(Tl) module was calculated by assuming the muon decays at uniform random positions in the crystal. Since cosmic-ray muons stop in the calorimeter randomly, the positron energy deposit in each module is common over all modules even in a complex structure of the calorimeter. This is a big advantage of the proposed calibration method. In contrast, in conventional calibration manners, the energy deposit depends strongly on the angle of cosmic rays, hit position, and the path length in the crystal. Therefore, it is very difficult to provide common calibration conditions to all calorimeter modules.

III. Experimental Proof Compared with Simulation

A. Setup

A schematic side view of the E36 experimental configuration is shown in Fig. 1. The gap veto counters located at the top of the E36 detector system were used as the trigger counters for cosmic-ray muons. Since a positron is emitted from the muon decay at rest, the signal waveform from the muon stopped CsI(Tl) module should have two pulses with a mean time interval of the muon life time of 2.2×10^{-6} s.

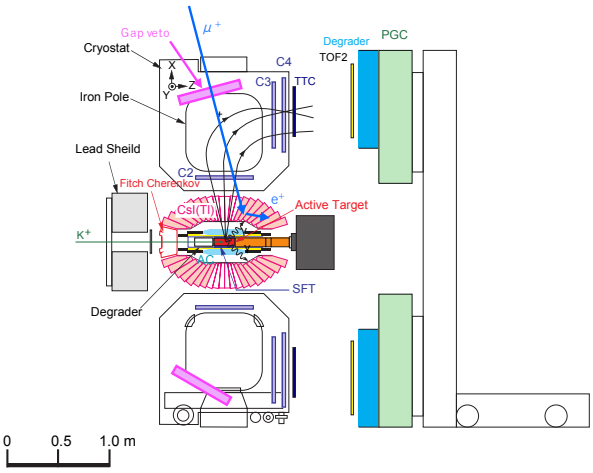

Fig. 1. Schematic side view of the detector apparatus for the J-PARC E36 experiment that was used to check the validity of the proposed calibration method using cosmic-ray muons.

B. Waveform Analysis

1) Model Function for the fitting: A typical waveform recorded in the flash ADC generated by the muon passage is shown in Fig. 2. The black dots are the experimental data and a red line is the fitted result. This model function can be described as,

$$F(t) = \frac{A}{f(t_0)} Freq\left(\frac{t-\tau_0-d}{\lambda}\right)\left\{\frac{t-\tau_0}{\tau_1} exp\left(1-\frac{t-\tau_0}{\tau_1}\right) + \varepsilon\frac{t-\tau_0}{\tau_2} exp\left(1-\frac{t-\tau_0}{\tau_2}\right)\right\}\theta(t-\tau_0)+v_0, \quad (2)$$

where A, τ_0, and v_0 are the pulse height amplitude, start time of pulses($\sim 1.02 \times 10^{-6}$ s), and base line, respectively. Also, d is the half-amplitude of the rise time ($\sim 1.10 \times 10^{-6}$ s), and λ is introduced to express the rise time width ($\sim 0.71 \times 10^{-6}$s). Two independent decay constants of τ_1 and τ_2 ($\sim 0.68 \times 10^{-6}$ s and $\sim 1.71 \times 10^{-6}$ s) and their amplitude ratio ε (~ 0.069) are adopted. $\theta(t)$ is a step function at $t = \tau_0$. The normalization factor, $f(t_0)$, is defined as,

$$f(t_0) = \frac{\varepsilon\tau_1(\varepsilon\tau_1+\tau_2)}{\varepsilon{\tau_1}^2+{\tau_2}^2} exp\left(1-\frac{\tau_1(\varepsilon\tau_1+\tau_2)}{\varepsilon{\tau_1}^2+{\tau_2}^2}\right) + \frac{\tau_2(\varepsilon\tau_1+\tau_2)}{\varepsilon{\tau_1}^2+{\tau_2}^2} exp\left(1-\frac{\tau_2(\varepsilon\tau_1+\tau_2)}{\varepsilon{\tau_1}^2+{\tau_2}^2}\right) \quad (3)$$

Here a cumulative distribution function of the Gaussian distribution, $Freq(x)$, is introduced to express the pulse shape in the rise time region,

$$Freq(x) = \int_x^\infty exp(-t^2/2)dt. \quad (4)$$

All these coefficients of the model function were extracted for each event with the least square method. The fitting performance was checked by using single pulse events.

2) Fitting residual: The general experimental wave forms could be tested with the fitting residual χ^2 of,

$$\chi^2 = \sum_t [F(t) - v(t)]^2, \quad (5)$$

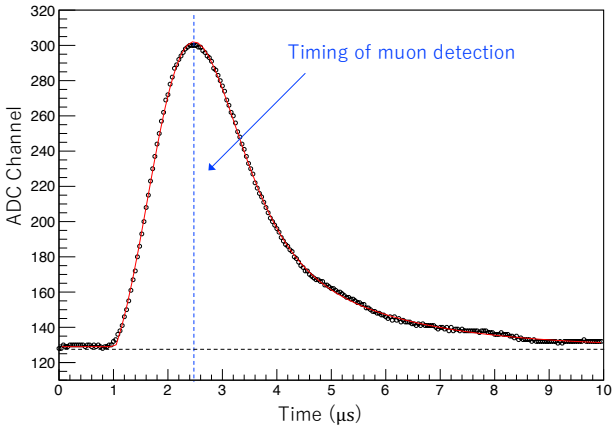

Fig. 2. A typical waveform from the flash ADC compared with the model function.

where $v(t)$ represents the data points and $F(t)$ the fitted model function for each waveform. A quadratic relationship between the χ^2 value and the pulse amplitude was observed in the single pulse case, as shown in Fig. 3, and this correlation was used to select multiple pulses in the observed waveform (Fig. 3).

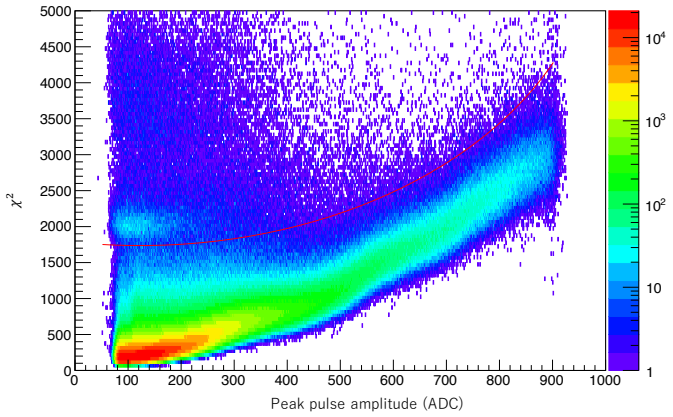

Fig. 3. Correlation plot of the peak height and the χ^2 value. The red line is the threshold level to select double-pulse waveforms.

3) Identification of the positron signal: The above fitting function was further developed to separate the first and second pulses in the double pulse waveform. The positron data were extracted by selecting events with large χ^2 values indicated by the red line in Fig. 3. The double-pulse waveform was reproduced by introducing the second pulse as a pileup to the first pulse in the model function, as shown in Fig. 4. The red, blue, and green lines are the fitted results, the muon and the positron contributions, respectively. The positron information such as the energy (E_{e^+}) and the time interval between the muon stop and positron emission (ΔT) was obtained by the two pulse fitting.

C. Monte Carlo Simulation by a GEANT4 code

A pure CsI crystal was adopted and the Tl component was neglected in a Monte Carlo (MC) simulation based on

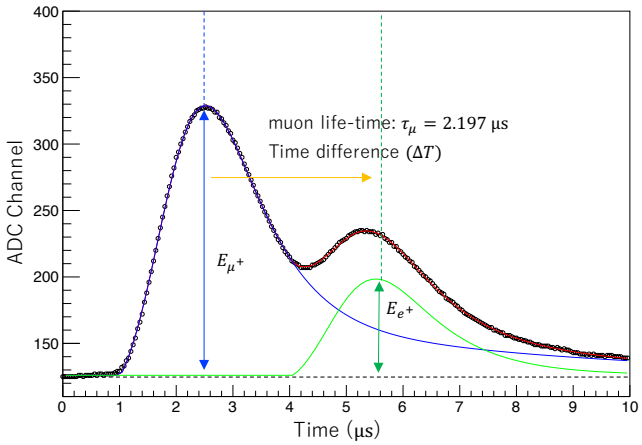

Fig. 4. A typical waveform of the positron emission event. The waveform was reproduced by introducing the second pulse as a pileup to the first pulse

a GEANT4 code version 10.02. The crystal shape assumed in the calculation is a trapezoid structure which is composed of a top area of 3 cm × 3 cm, a bottom area of 6 cm × 6 cm, and a height of 25 cm. Muons are assumed to be uniformly distributed in the crystal and decay at rest ($\mu^+ \rightarrow e^+\nu_e\bar{\nu_\mu}$), and an absolute energy deposit could be calculated reliably using this code. Also its validity could be confirmed using the energy deposit of $K_{\mu 2}$ muon confined in a crystal. The shower leakage from the crystal was taken into account and the introduces significant energy shift of the Michel spectrum to the lower energy region.

It is known that μ^+ and μ^- yields of lower-energy cosmic muons are almost the same and most of the μ^-s are capture by nuclei ($\mu^- p \rightarrow n\nu_\mu$) without emitting secondary electrons. Therefore, the energy deposit from the μ^- decay is mainly contributed from a recoil daughter nuclei and gamma rays from neutron capture states. The energy distributions calculated by generating μ^+ and μ^- in the crystal is shown in Fig. 5, as indicated by the blue and red histograms, respectively. Also, for calibration purposes, the energy distributions without considering the shower leakage from the crystal are shown in the figure, as indicated by black histogram for μ^+ and green histogram for μ^-. In the actual E36 model system, the μ^+ spectrum is dominant in the region of $20-53$ MeV. Therefore, the endpoint energy can be determined to be 53 MeV even if the μ^- contribution is uncertain.

D. Results

The time interval spectrum between the $\mu^+(\mu^-)$ and $e^+(e^-)$ is shown in Fig. 6. The black and white dots are the experimental data obtained by selecting events in $20-40$ and $20-80$ MeV, respectively. The decay constants of an exponential function were derived to be $(2.07 \pm 0.03) \times 10^{-6}$ s and $(2.10 \pm 0.04) \times 10^{-6}$ s, for events in the region of $20-40$ and $20-80$ MeV, respectively. They are consistent with the muon lifetime, indicating a small contribution from the μ^- decays

The double-pulse separation efficiency for events with $\Delta T < 4 \times 10^{-6}$ s significantly decreased because the fitting

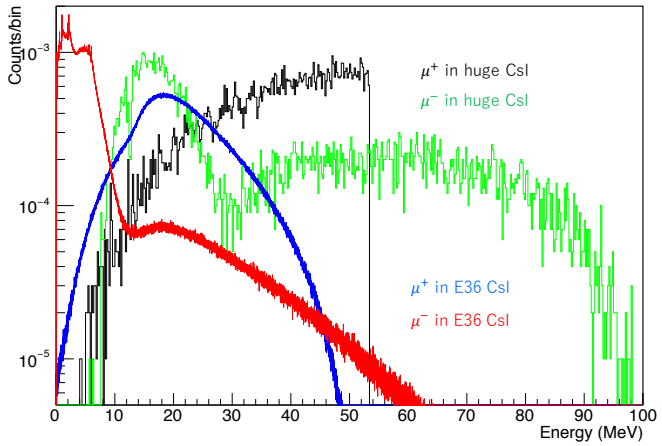

Fig. 5. Muon energy deposit in the crystal calculated by a GEANT4 code with/without taking into account the shower leakage from the crystal.

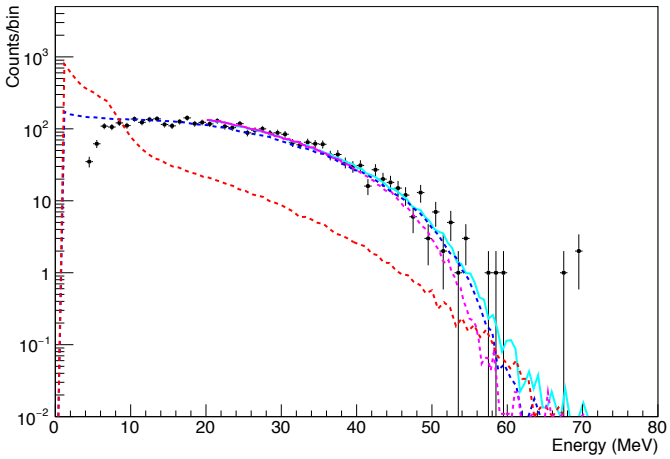

Fig. 7. Energy spectrum of the second pulses. The experimental results were compared with the simulation and the endpoint energy was determined by taking into account the μ^+ and μ^- contributions.

was not successful due to unclear second pulses. Thus, the double-pulse waveforms with $\Delta T > 4 \times 10^{-6}$ s were selected to the energy distribution.

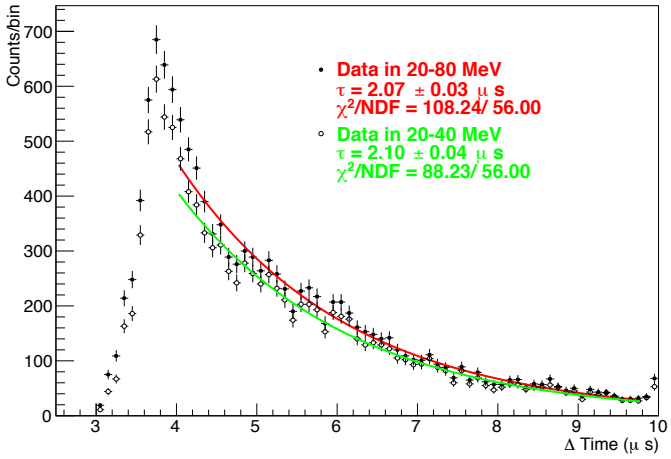

Fig. 6. The μ/e time difference spectrum. The decay constants were obtained to be $(2.07 \pm 0.03) \times 10^{-6}$ s and $(2.10 \pm 0.04) \times 10^{-6}$ s, for events in the region of $20 - 40$ and $20 - 80$ MeV, respectively.

The black dots in Fig. 7 show the $e^+(e^-)$ energy distribution. The experimental results were compared with the simulation, as shown in the blue (μ^+) and red (μ^-) lines. An endpoint energy of 53.20 ± 0.04 MeV(0.08%) was successfully determined using events in the region of $20 - 40$ MeV (magenta line). The good fitting result of $\chi^2/NDF = 18.85/19$ indicates this method is applicable and leads to consistent results with conventional calibrations. The analysis was repeated using events in the region of $20 - 80$ MeV (cyan line) adding the μ^- contribution. However, the endpoint energy was determined to be 55.33 ± 0.04 MeV under the assumption of the ratio of $\mu^+/\mu^- = 1$ ($\chi^2/NDF = 39.023/39$). This deterioration is interpreted that the μ^- contribution has not been understood correctly in the region of higher than 50 MeV where the μ^- contribution should be dominant.

IV. Conclusion

The energy calibration of the CsI(Tl) calorimeter in the J-PARC E36 experiment was performed with a newly developed method using stopped cosmic-ray muons. The positron signal of muon decay in the crystal could be observed as a second pulse in the flash ADC waveform. The energy spectrum of this second pulse could be well reproduced with the simulated energy deposit of the Michel spectrum. The energy end point of the second signal can be thus used as the calibration point of 53.2 MeV. This versatile calibration scheme can be applied to any calorimeters.

References

[1] S. Strauch for the TREK collaboration, " Searches for New Physics with the TREK Detector", PoS(KAON13)014.

[2] Particle Data Group, " REVIEW OF PARTICLE PHYSICS", Chinese Physics C Vol. 38, No. 9 (2014) 090001.

[3] V. Cirigliano, G. Ecker, H. Neufeld, A. Pich, and J. Portoles, " Kaon Decay in the Standard Model", Rev. Mod. Phys. 84, pp. 399, 2012.

[4] C. Lazzeroni for the NA62 collaboration, " Precision Measurement of the Ratio of the Charged Kaon Leptonic Decay Rates", Phys. Lett. B719, pp. 326-336, 2013.

[5] P. Depommier, "Search for non-standard time-reversal violation", Nucl. Phys. A, Vol. 654, Issue 1, pp. 935c-938c, 1999.

[6] M. Tabata, A. Toyoda, H. Kawai, Y. Igarashi, J. Imazato, S. Shimizu, and H. Yamazaki," Fabrication of silica aerogel with $n = 1.08$ for e^+/μ^+ separation in a threshold Cherenkov counter of the J-PARC TREK/E36 experiment", Nucl. Instrum. Methods A, Vol. 795, pp. 206-212, 2015.

[7] O. Mineev, Y. Kudenko, N. Yershov, S. Bianchin, M. Hasinoff, K. Horie, S. Shimizu, Y. Igarashi, J. Imazato, A. Toyoda, H. Ito, H. Kawai, S. Kodama, and M. Tabata, " A Spiral Fiber Tracker for the J-PARC E36 experiment", Proc. Sci., PoS(PhotoDet2015) 069.

[8] Y. Miyazaki, S. Shimizu, S. Bianchin, C. Djalali, D. Gill, J. Jian, M. Hasinoff, K. Horie, Y. Igarashi, J. Imazato, A. Ivashkin, M. Kohl, R. Narikawa, R. Pywell, S. Strauch, M. Tabata, A. Toyoda, H. Yamazaki, and T. Yoshioka, " Performance test of a lead-glass counter for the J-PARC E36 experiment", Nucl. Instrum. Methods At Vol. 779, pp. 13-17, 2015.

[9] Yu.G. Kudenko, O.V. Mineev, J. Imazato, " Design and performance of the readout electronics for the CsI(T1) detector ", Nucl. Instrum. Methods A, Vol. 411, pp. 437-448, 1998.